IEEE Access
Multidisciplinary : Rapid Review : Open Access Journal

Received October 21, 2021, accepted November 1, 2021, date of publication November 11, 2021,
date of current version November 22, 2021.

Digital Object Identifier 10.1109/ACCESS.2021.3127221

A Method of Camera Calibration Based on Kriging Interpolation

CHUANG LIU, QIUCHENG SUN, WEIYU DAI, ZEMING REN, QINGLIANG LI, AND FANHUA YU
College of Computer Science and Technology, Changchun Normal University, Changchun 130032, China
Corresponding author: Qiucheng Sun (sunqiucheng@mail.ccsfu.edu.cn)

This work was supported in part by the Foundation of Jilin Provincial Education Department under Grant JJKH20190499KJ; and in part by the Foundation of Jilin Provincial Development and Reform Commission under Grant 2019C039-1, Grant 2019C054, and Grant 2020C019-3.

ABSTRACT The basis of visual measurement is camera calibration. In the traditional calibration method, the radial and tangential distortion models usually are adopted. Because of the randomness of lens distortion, the above fixed form distortion model cannot accurately express the distortion distribution. To solve the above problems, a calibration method with a new distortion model is presented in the paper. First, an exact linear model is obtained, using only the corner coordinates of the image center region; then, using this model, the projection deviation of all corner points in the pixel plane can be obtained, that is, the point cloud of projection deviation distribution; finally, the Kriging interpolation method is used to obtain a continuous projection deviation distribution function which can accurately express lens distortion in the pixel plane. Using this function and the corresponding linear model, all two-dimensional image points can be accurately projected into three-dimensional space. To compare with the traditional method, the mean error of projection and measurement error are calculated in the experiment, and the experimental results show that the calibration method is more accurate and more suitable for measuring requirements.

INDEX TERMS Camera calibration, distortion model, kriging interpolation.

I. INTRODUCTION

Camera calibration is the process of solving the internal and external parameters and distortion coefficient of the camera by the three-dimensional coordinates of the space target point and its two-dimensional projection coordinates [1]–[7]. Camera calibration is a key step in machine vision, and its accuracy has a direct impact on the measurement accuracy of the vision system [8].

Up to now, camera calibration methods can be divided into two types, which are the target-based calibration methods and the self-calibration methods. However, the self-calibration method has some limits in practical measurements, and the calibration accuracy is relatively low. Thus, we focus on the target-based calibration method here. A two-step calibration method based on the targets is proposed by Tsai in [9]. The classic two-step method is concise in the process, but has a low accuracy. Weng proposed a camera model with three kinds of distortion, which can adapt to the lens distortion [10]–[12]. A more simple, flexible, and high-accuracy method was proposed by Zhang, in which a non-linear method is used to solve the distortion parameters [13]. This method does not require an expensive calibration model and is therefore highly practical. Since then, camera calibration methods and theories have been widely used. Most of the present calibration methods are based on the Zhang's camera model. Bradley and Heidrich presented a method, which uses a rectification error to calibrate camera accurately [14]. Yannick Hold-Geoffroy and Yao use a convolutional neural network for camera calibration, and internal and external parameters and distortion coefficient of the camera can be precisely solved [15], [16]. A geometry-based camera calibration technique is proposed by Jen-Hui Chuang in [17], which improves the speed of solving the model parameters. These calibration methods are based on the principle of using small-aperture imaging and fixed models, which optimize for different initial value solving methods and improve accuracy. Since distortions are an inherent property of the lens and the optimization of the initial values only by the fixed form model, the improved accuracy is

The associate editor coordinating the review of this manuscript and approving it for publication was Amin Zehtabian.

limited. Therefore, many scholars have improved the calibration accuracy by correcting the lens distortion of the camera.

Conrady proposed a famous model in which he classified lens distortions into radial and tangential distortion, and suggested the calibration of these distortions using the plumb-line method [18], [19]. The model has been widely used since then [10], [20]. The literature [21] has made some mathematical changes to the model. Subsequently, a non-parametric radial distortion model has been proposed in [22], but it only applies radial distortion. Although radial distortion accounts for most of the lens distortion, it is not enough for industries that require high accuracy. In the literature [23], three different models were used to calibrate different regions and better results were obtained. Lens distortion was corrected by using a digital image correlation method in [24]. Since camera distortion is random due to lens manufacturing errors, the above traditional methods use a fixed form of distortion model, which does not accurately describe the distribution of distortion [25], [26].

Thus, a method of camera calibration based on Kriging interpolation is proposed in this paper. In the present work, the camera parameters with the distortion-free camera model is obtained by improved Zhang's method, which only uses the central region points of the image. Then, the image distortion is corrected using the Kriging interpolation method. Finally, a method of measuring the distance is proposed by using the parallel line to test the accuracy and performance of the method. This paper is organized as follows: A linear calibration model is proposed in Section II. In Section III, a distortion model based on Kriging interpolation is presented. A computer simulation experiment and a method of measuring planar dimensions is given to verify the correctness of our method in Section IV. The conclusions of this paper are presented in Section V.

II. LINEAR MODEL

Currently, camera calibration usually uses the method of the literature [13], which maps a 3D spatial scene onto a 2D camera image plane. Considering the radial and tangential distortions, the mapping model of world coordinates to pixel coordinates can be expressed as:

$$\begin{bmatrix} X_c \\ Y_c \\ Z_c \end{bmatrix} = R \begin{bmatrix} X_w \\ Y_w \\ Z_w \end{bmatrix} + T \rightarrow \begin{bmatrix} x_u \\ y_u \end{bmatrix} = \frac{1}{Z_c} \begin{bmatrix} X_c \\ Y_c \end{bmatrix} \tag{1}$$

$$\begin{aligned} \begin{bmatrix} x_d \\ y_d \end{bmatrix} &= \left(1 + k_1 r^2 + k_2 r^4\right) \\ &\quad \times \begin{bmatrix} x_u \\ y_u \end{bmatrix} \begin{bmatrix} 2p_1 x_u y_u + p_2\left(r^2 + 2x_u^2\right) \\ p_1\left(r^2 + 2y_u^2\right) + 2p_2 x_u y_u \end{bmatrix} \end{aligned} \tag{2}$$

$$\begin{bmatrix} u_p \\ v_p \\ 1 \end{bmatrix} = \begin{bmatrix} \alpha & \gamma & u_0 \\ 0 & \beta & v_0 \\ 0 & 0 & 1 \end{bmatrix} \begin{bmatrix} x_d \\ y_d \\ 1 \end{bmatrix} \tag{3}$$

where $r = \sqrt{x_u^2 + y_u^2}$, k_1 and k_2 are radial distortion parameters, p_1 and p_2 are tangential distortion parameters. The final nonlinear optimization is completed using LM(Levenberg-Marquardt) algorithm.

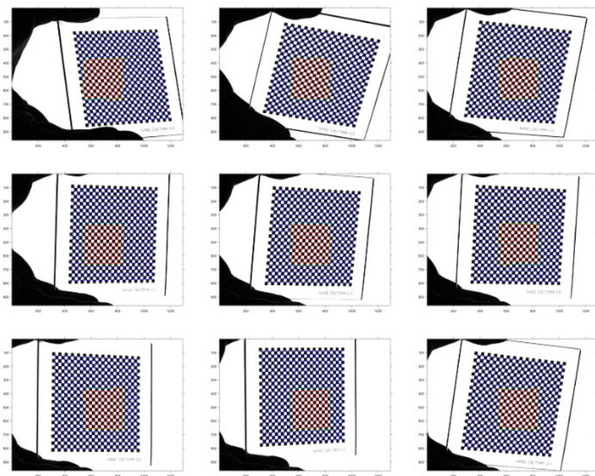

FIGURE 1. Calibration images.

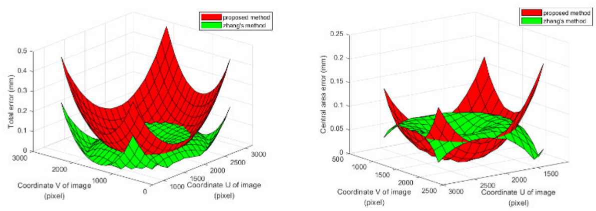

(a) Overall error comparison (b) Comparison of centre error

FIGURE 2. The projection error of Zhang and proposed methods.

According to the literature [27], it is known that the camera is affected by lens distortion in the projection centre region is relatively small. In proposed method only the feature points in the area around the projection centre are used for calibration, as are shown in the red area of 400 × 400 in Figure.1, so that the influence of distortions can be ignored. Then calibration model (1-3) can be simplified to the following form:

$$s \begin{bmatrix} u_p \\ v_p \\ 1 \end{bmatrix} = A \begin{bmatrix} r_1 & r_2 & t \end{bmatrix} \begin{bmatrix} X_w \\ Y_w \\ 1 \end{bmatrix} = H \begin{bmatrix} X_w \\ Y_w \\ 1 \end{bmatrix} \tag{4}$$

In the equation (4), $Z_w = 0$, (u_p, v_p) represents the undistorted pixel coordinates, (X_w, Y_w) represents for the world coordinates, $r_i(\mathrm{i} = 1, 2)$ is the ith column vector of the rotation matrix, t is the translation vector, the internal reference matrix A $= \begin{bmatrix} \alpha & \gamma & u_0 \\ 0 & \beta & v_0 \\ 0 & 0 & 1 \end{bmatrix}$, and the homographic H is a 3×3 matrix.

Using the corner data in Figure. 1, the calibration of Zhang's and proposed method is completed respectively. As is shown in Figure. 2, the projection error distribution of two methods from the pixel plane to 3D space is given, where the error is the distance between the projection point and the real 3D point. It can be seen that in the central region of the image, Zhang's projection deviation is larger, whereas it is smaller in this paper. However, the projection deviation outside the central region shows the opposite result. It indicates that Zhang's distortion model is a fixed form model based on fitting form and will be affected by all calibration points. As the calibration image points gradually move away from the central region, the distortion function becomes more influenced by the calibration image points outside of the central region. These points are usually severely distorted, which can sacrifice the calibration accuracy in the central region. As for the method in this paper, since only the corner points within the central region (400 × 400) are used for calibration, the projection deviation in the central region is relatively small, whereas the deviation out of the central region is relatively large. In practical applications, it is not sufficient to complete the calibration and measurement using only the central region. Therefore, to overcome the shortcoming of the existing distortion model, a new distortion model will be given in the following section.

III. DISTORTION MODEL

Lens distortion is an inherent property of the cameras, and it is difficult to eliminate through physical methods, but it can be corrected by mathematical methods. Since there is randomness in the distribution pattern of distortion error, the traditional distortion modes are often not able to accurately describe the distortion. Meanwhile, the traditional distortion models are usually obtained based on fitting, and the model will be affected by large detection error in the process of solving. Therefore, an image distortion model based on Kriging interpolation is proposed in this paper.

A. ANALYSIS OF PROJECTION DEVIATION

Using the method in Section II of this paper, the world coordinates corresponding to the corner points of the check board can be projected as pixel coordinates, which will be considered as ideal pixel coordinates. In real imaging systems, due to the prevalence of lens distortion, the image will be distorted by the deviation between the ideal pixel coordinates and the actual pixel coordinates detected by the corner point detection algorithm, which can be expressed by the following equation:

$$\delta_m = m_1 - m_0 \tag{5}$$

where m_1 represents the actual pixel coordinates of the corner point, m_0 represents the ideal pixel coordinates calculated using Equation (4), δ_m represents the deviation between the Ideal pixel coordinates and the actual pixel coordinates, which is composed of two parts together: δ_u (deviation in the U-direction) and δ_v (direction in the V-direction). Using the actual pixel coordinates u_d and v_d of the corner point as U and V respectively, the scatter plot of two three-dimensional deviation distribution can be obtained by using one of δ_u or δ_v as Z value, the deviations obtained through the single images are shown in Figures 3,4.

These scatter points only describe the pixel distortion deviation corresponding to the corner points of the check board,

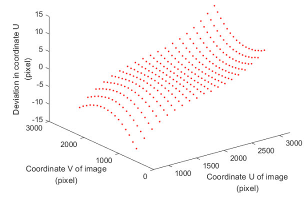

FIGURE 3. Projection deviation in U-direction.

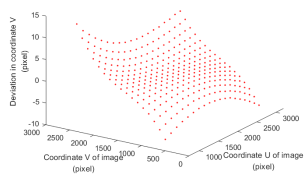

FIGURE 4. Projection deviation in V-direction.

which do not reflect the pixel distortion deviation corresponding to any pixel points in the whole pixel plane. Therefore, the above scatter map is interpolated into a continuous deviation correction surface by using Kriging interpolation in this paper, so as to obtain a continuous distortion function.

B. KRIGING INTERPOLATION PRINCIPLE

In order to more accurately describe the lens distortion of the camera, through the known scatter point data, find the trend in the data and predict the points in the unknown region, according to this trend, this method of predicting the points according to a certain data trend can be done with Kriging interpolation.

The Kriging interpolation method, in a statistical sense, is a method for unbiased and optimal estimation of the values taken by the regionalized variables in a finite region, starting from the correlation and variability of the variables. The ordinary Kriging function satisfies the second-order smoothness assumption and the intrinsic assumption that the regionalized variable $Z(x)$ consists of two components, the expectation m and the residual $e(x)$, as is shown in (6).

$$Z(x) = m + e(x) \tag{6}$$

where the expectation m is unknown and the expectation of the residual $e(x)$ is 0. The second-order smooth assumption of the variable $Z(x)$ is:

$$\begin{aligned} E\left[Z(x+h) - Z(x)\right] &= 0 \\ Var\left[Z(x+h) - Z(x)\right] &= 2\gamma(h) \end{aligned} \tag{7}$$

where $\gamma(h)$ is the proposed variable function based on the spatial variability structure or the spatial continuity of the random variable, the value $\gamma(h)$ can be calculated in the case of the limited sample. As in equation (8):

$$\gamma(h) = \frac{1}{2N_h} \sum_{i=1}^{N_h} \left[Z(x_i + h) - Z(x_i)\right]^2 \tag{8}$$

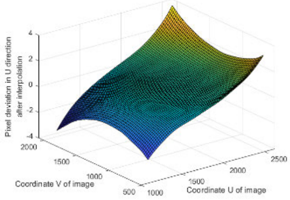

FIGURE 5. U-direction deviation correction surface.

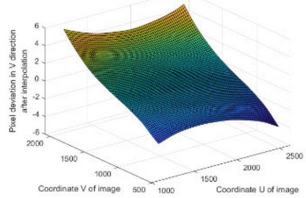

FIGURE 6. V-direction deviation correction surface.

where N_h means the number of sample pairs used to calculate the value of the variable function of the n-dimensional space sample, the subscript h indicates that N_h is a function related to the distance h. $Z(x_i + h)$ refers to the value of the random variable, which deviates from the point x_i by a distance h, $Z(x_i)$ indicates the value of the random variable at x_i, and h is the spatial interval distance of the sample points. The estimation formula for the Kriging estimation method is:

$$\hat{z}(x_0) = \sum_{i=1}^{n} \lambda_i z(x_i) \tag{9}$$

$z(x_i)$ is the known value of the random function at (x_i, y_i) whereas $\hat{z}(x_0)$ is the estimation of the random function at (x_0, y_0). λ_i is a set of weight coefficients at the ith point and n is the number of observed values used for estimation. Satisfying the $\hat{z}_0$ estimate of unbiased and when the variance of estimation error is minimized, with the aid of Lagrange multipliers and performing extreme value operations, the derivation leads to the Kriging equations.

$$\begin{cases} \sum_{i=1}^{n} \lambda_i \gamma\left(x_i, x_j\right) + \mu = \gamma\left(x_j, x_0\right), j = 1, \ldots, n \\ \sum_{i=1}^{n} \lambda_i = 1 \end{cases} \tag{10}$$

Its matrix form is:

$$\begin{bmatrix} \gamma_{11} & \ldots & \gamma_{1n} & 1 \\ \vdots & \ldots & \ldots & \vdots \\ \gamma_{n1} & \ldots & \gamma_{nn} & 1 \\ 1 & \ldots & 1 & 0 \end{bmatrix} \begin{bmatrix} \lambda_1 \\ \vdots \\ \lambda_n \\ \mu \end{bmatrix} = \begin{bmatrix} \gamma_{01} \\ \vdots \\ \gamma_{0n} \\ 1 \end{bmatrix} \tag{11}$$

where $\gamma_{ij} = \gamma(x_i - x_j)$, represents that the distance is the value of the variance function between x_i and x_j. Both the left coefficient matrix and the vector to the right of the equal sign are known, so the system of linear equations can be solved to obtain the weights $\lambda_i(i = 1, \ldots, n)$ and the Lagrange multiplier μ. The above introduction to Kriging interpolation theory allows a reasonable addition to the data for unknown regions based on existing data.

In this paper, we use functions to describe the lens distortion surface and use interpolation functions to correct the image distortion. By comparing with other kriging methods, the ordinary kriging interpolation method is more efficient in fitting and the deviation surface obtained is smoother, which can describe the lens distortion better, so in this paper, the ordinary kriging interpolation method is used for camera calibration.

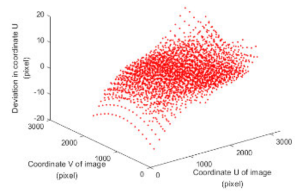

FIGURE 7. Projection deviation of Multiple images in U direction.

C. THE KRIGING-BASED MODEL DISTORTION FUNCTION

The distortion correction function can be solved in the pixel plane by combining the scatter points in A of III and the Kriging interpolation theory in B of III. The corner point detection algorithm in the literature [28] is used to detect the corner points of a set of calibration board images as raw data, and the deviation correction surface is generated by combining the kriging interpolation function. The initial parameters passed into the interpolation model are the actual pixel coordinates u_d and v_d, in addition the δ_u, which allows to obtain the deviation correction function about the U direction. Similarly, the deviation correction function in V direction can be obtained, as are shown in Figures 5 and 6. Finally, the generated continuous function can be used to achieve error correction for arbitrary pixel points. The correction forms are as follows:

$$\begin{aligned} u_p &= u_d + \delta_u\left(u_d, v_d\right) \\ v_p &= v_d + \delta_v\left(u_d, v_d\right) \end{aligned} \tag{12}$$

where u_p and v_p are the pixel coordinates after correction, which are the ideal image coordinates. The δ_u and δ_v in Eq. (12) can be described by the interpolation function as follows.

$$\begin{aligned} \delta_u &= f_u\left(u_d, v_d\right) \\ \delta_v &= f_v\left(u_d, v_d\right) \end{aligned} \tag{13}$$

where f_u and f_v are the Kriging interpolation function of the adapted surfaces.

According to the multiple calibration images, several sets of δ_u and δ_v values are obtained, and all the deviations are projected into two three-dimensional spatial coordinate systems to obtain deviation correction surfaces generated by the above method, as are shown in Figures 7 and 8, which are then interpolated.

In order to obtain surfaces that accurately the lens distortion, all surfaces are obtained by using a fitting method, as are

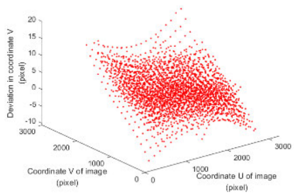

FIGURE 8. Projection deviation of Multiple images in V direction.

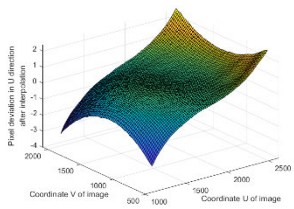

FIGURE 9. U-direction deviation correction surface.

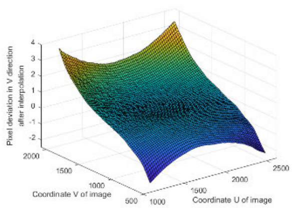

FIGURE 10. V-direction deviation correction.

shown in Figures 9 and 10. In this way, the error caused by using a single surface to represent the distortion can be averaged.

The flow chart of the proposed camera calibration method in this paper is given, as is shown in Figure 11.

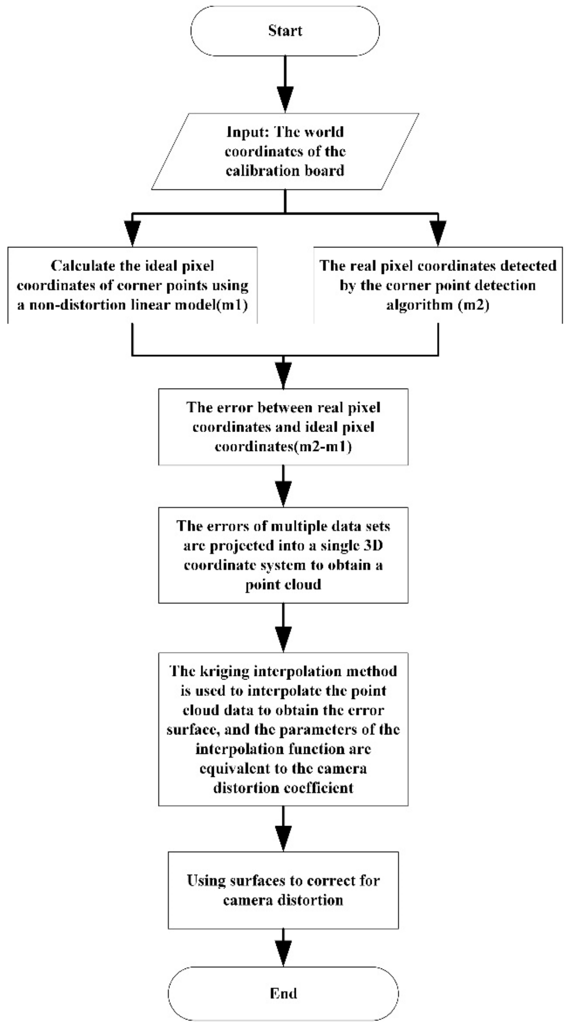

FIGURE 11. Flow chart of proposed method.

IV. EXPERIMENT

A. RESIDUAL COMPARISON OF PROJECTION

In the experiment, the camera is a MER-125-30UM model camera produced by DAHENG Image, whose image resolution is 3840 pixels $\times$ 2784 pixels. A 25mm fixed-lens camera is used to capture nine patterns of a check board, as is shown in Figure 1. The size of the check board grid is 4×4 mm, and the method in [28] is used to detect the corner points in the image. According to the method proposed in this paper, the camera is calibrated by (4) using the corner points in the 400×400 area around the image projection center, and then the distorted pixel points are corrected by a deviation correction surface to complete the calibration experiment. The corrected pixel points are projected into the world coordinate system using the linear model (4), and the error between the projected points and the actual world coordinates are calculated. The formula is as follows:

$$E_{ij} = ||M - \hat{M}_{ij}||_2, \quad i= 1, \ldots, m,\ j= 1, \ldots, n \tag{14}$$

where $||\cdot||$ is the second paradigm of the vector, i denotes the number of corner points for each picture, j indicates the number of the pictures. The point E_{ij} is the error corresponding to each calibrated picture.

The above process is repeated 9 times, each time the camera is calibrated with 9 patterns. For comparison purposes, the experiments also give the projected errors which use the Zhang's calibration method for the same data, and the experimental results are listed in Table 1.

From the experimental data in Table 1, it can be seen that the maximum projection error calculated by the proposed method is less than $1.6099e^{-12}mm$ and the average projection error is less than $7.1962e^{-14}mm$; the maximum projection error of Zhang's is less than $0.2320mm$ and the average projection error is less than $0.0063mm$. Further statistics show that the mean projection error of the proposed method in each experiment is about $5.9408e^{-14}mm$. By comparing the root mean square (RMS), the proposed method is better than Zhang's calibration method, with less dispersion of the data.

B. PARALLEL LINE DISTANCE MEASUREMENT METHOD

In the traditional calibration method, the objective function is usually the squared sum of the projected errors in all the

TABLE 1. The projected errors.

NO	Zhang's method(mm)		Proposed method(mm)	
	Max	Average	Max	Average
1	0.1116	0.0046	$7.7276e^{-13}$	$4.1780e^{-14}$
2	0.2320	0.0063	$1.2984e^{-13}$	$3.2497e^{-14}$
3	0.2203	0.0056	$1.2674e^{-13}$	$4.1258e^{-14}$
4	0.1500	0.0043	$6.3917e^{-14}$	$4.7554e^{-14}$
5	0.0954	0.0045	$9.5956e^{-13}$	$7.1962e^{-14}$
6	0.1686	0.0048	$7.1563e^{-13}$	$6.4258e^{-14}$
7	0.2015	0.0060	$2.0349e^{-13}$	$5.2558e^{-14}$
8	0.0905	0.0043	$1.6099e^{-12}$	$1.0162e^{-14}$
9	0.1892	0.0050	$9.1921e^{-13}$	$5.1008e^{-14}$
Average	0.1621	0.0051	$6.1122e^{-13}$	$5.6055e^{-14}$
RMS	0.1698	0.0051	$7.8493e^{-13}$	$5.9408e^{-14}$

corner point coordinates, which is minimized in the optimization process. However, it is not sufficient to measure the accuracy of the calibration method by only the inverse projection error of the corner point coordinates, more points should be used as a basis for measuring the accuracy of the calibration. Then, a parallel line ranging method is proposed, measurement the known distance of two sides of the square on the check board, to evaluate the accuracy of different calibration methods. The specific steps of the method are as follows:

(1) Nine calibration check board images are used to complete the calibration of the proposed method and Zhang's method respectively. The intrinsic matrix A_{mine} and A_{zhang} are as follows.

$$A_{mine} = \begin{bmatrix} 5.0721e^{+03} & -1.5678 & 1.9639e^{+03} \\ 0 & 5.0701e^{+03} & 1.3201e^{+03} \\ 0 & 0 & 1 \end{bmatrix},$$
$$A_{zhang} = \begin{bmatrix} 4.9437e^{+03} & -2.4154 & 1.9506e^{+03} \\ 0 & 4.9459e^{+03} & 1.3370e^{+03} \\ 0 & 0 & 1 \end{bmatrix}.$$

(2) Select one of the calibrated images as measured image, the rotation matrix are

$$R_{mine} = \begin{bmatrix} 0.9917 & -0.0242 & -0.1266 \\ 0.0263 & 0.9995 & -0.0155 \\ -0.1262 & 0.0187 & 0.9918 \end{bmatrix}$$

and

$$R_{zhang} = \begin{bmatrix} 0.9918 & -0.0240 & 0.1259 \\ 0.0268 & 0.9994 & -0.0209 \\ -0.1253 & 0.0241 & 0.9918 \end{bmatrix},$$

the translational vector are

$$T_{mine} = \begin{bmatrix} -37.6149 \\ -27.4417 \\ 165.5312 \end{bmatrix} \text{ and } T_{zhang} = \begin{bmatrix} -37.1987 \\ -27.9862 \\ 162.1240 \end{bmatrix}.$$

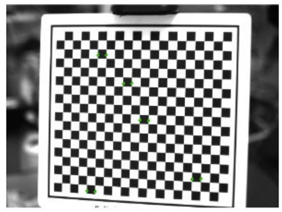

FIGURE 12. Parallel line ranging.

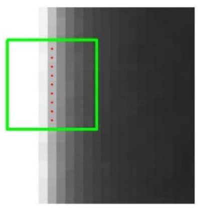

FIGURE 13. Window corner point detection.

The edge detection algorithm of the literature [29], [30] is used to detect any two edges of the square in the image, as is shown in Figure 12. The effect of corner point detection is shown in Figure 13. The pixel coordinates of the square edges are projected to world coordinates form the calibration data of the two above calibration methods.

(3) The two lines lie in the same plane of the world coordinate system (Z = 0), then the world coordinates of the edge points can be fitted in the world coordinate system. The equations of the parallels are as follows.

$$\begin{aligned} L_1 &: Ax + By + C_1 = 0, \quad Z = 0 \\ L_2 &: Ax + By + C_2 = 0, \quad Z = 0 \end{aligned} \tag{15}$$

The whole measurement can be represented in Figure 14, where the square is one of the check board grids in the picture, and its true distance $d = |C_1 - C_2| / \sqrt{A^2 + B^2}$ is the distance between L1 and L2 on the measurement plane.

TABLE 2. Parallel line ranging results.

Measurement methods	Number of measurements						MAE	RMS
	1	2	3	4	5	6		
Zhang	3.8297	4.0146	3.9009	4.0323	4.0184	3.9311	0.0673	0.0868
proposed	3.9506	4.0097	3.9508	4.0113	3.9964	3.9603	0.0271	0.0333

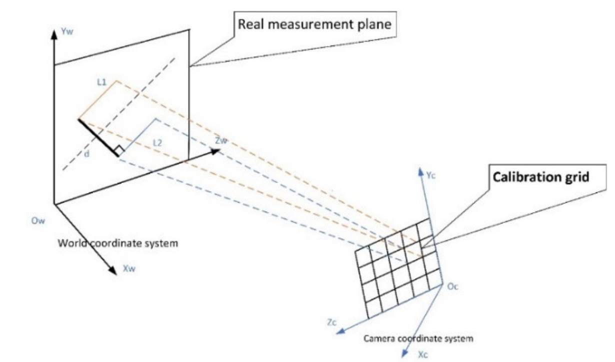

FIGURE 14. Parallel line detection principle.

The experiment is repeated to obtain multiple sets of experimental data, and the results are listed in Table 2. It is shown that the mean absolute error (MAE) of the proposed method is 0.0271 mm whereas Zhang's method is 0.0673 mm. The RMS error is 3.9552 mm and 3.9799 mm respectively. The experimental results show that the method proposed in this paper has a high measurement accuracy.

V. CONCLUSION

To improve the calibration accuracy, a new distortion model is proposed. Different from the previous models, the randomness of distortion distribution is fully considered. In this paper, the correction surface is obtained by Kriging interpolation, which can accurately describe the distortion distribution of a camera. In the experiment, compared with the traditional method, the calibration method has been directly verified to improve the measurement accuracy. This method is more suitable for correction of lens with large distortion, such as fish eyes.

REFERENCES

[1] Z. Liu, Q. Wu, S. N. Wu, and X. Pan, "Flexible and accurate camera calibration using grid spherical images," *Opt. Exp.*, vol. 25, no. 13, pp. 15269–15285, Aug. 2017.

[2] J. Sun, M. M. Hossain, C.-L. Xu, B. Zhang, and S.-M. Wang, "A novel calibration method of focused light field camera for 3-D reconstruction of flame temperature," *Opt. Commun.*, vol. 390, pp. 7–15, May 2017.

[3] J. A. Munoz-Rodriguez, R. Rodriguez-Vera, and M. S. Guirado, "Direct object shape detection based on skeleton extraction of a light line," *Opt. Eng.*, vol. 39, no. 9, pp. 2463–2471, 2000.

[4] J. A. M. Rodríguez, "Calibration modeling for mobile vision based laser imaging and approximation networks," *J. Modern Opt.*, vol. 57, no. 17, pp. 1583–1597, Oct. 2010.

[5] J. A. Muñoz-Rodríguez, A. Asundi, and R. Rodríguez-Vera, "Shape detection of moving objects based on a neural network of a light line," *Opt. Commun.*, vol. 221, nos. 1–3, pp. 73–86, Jun. 2003.

[6] J. Rodríguez, R. Rodriguez-Vera, and A. Asundi, "Depth object recovery using a light line and a regression neural network," *Optica Applicata*, vol. 35, no. 2, pp. 1–15, 2005.

[7] J. A. M. Rodríguez, R. Rodríguez-Vera, A. Asundi, and G. G. Campos, "Shape detection using light line and Bezier approximation network," *Imag. Sci. J.*, vol. 55, no. 1, pp. 29–39, Mar. 2007.

[8] Z. Jia, J. Yang, W. Liu, F. Wang, Y. Liu, L. Wang, C. Fan, and K. Zhao, "Improved camera calibration method based on perpendicularity compensation for binocular stereo vision measurement system," *Opt. Exp.*, vol. 23, no. 12, pp. 15205–15223, 2015.

[9] R. Y. Tsai, "A versatile camera calibration technique for high-accuracy 3D machine vision metrology using off-the-shelf TV cameras and lenses," *IEEE J. Robot. Autom.*, vol. JRA-3, no. 4, pp. 323–344, Aug. 1987.

[10] J. Weng, P. Cohen, and M. Herniou, "Camera calibration with distortion models and accuracy evaluation," *IEEE Trans. Pattern Anal. Mach. Intell.*, vol. 14, no. 10, pp. 965–980, Oct. 1992.

[11] J. Weng, P. Cohen, and M. Herniou, "Calibration of stereo cameras using a non-linear distortion model (CCD sensory)," in *Proc. 10th Int. Conf. Pattern Recognit.*, vol. 1, 1990, pp. 246–253.

[12] J. Weng, P. Cohen, and N. Rebibo, "Motion and structure estimation from stereo image sequences," *IEEE Trans. Robot. Autom.*, vol. 8, no. 3, pp. 362–382, Jun. 1992.

[13] Z. Zhang, "A flexible new technique for camera calibration," *IEEE Trans. Pattern Anal. Mach. Intell.*, vol. 22, no. 11, pp. 1330–1334, Nov. 2000.

[14] D. Bradley and W. Heidrich, "Binocular camera calibration using rectification error," in *Proc. Can. Conf. Comput. Robot Vis.*, 2010, pp. 183–190.

[15] Y. Hold-Geoffroy, K. Sunkavalli, J. Eisenmann, M. Fisher, E. Gambaretto, S. Hadap, and J.-F. Lalonde, "A perceptual measure for deep single image camera calibration," in *Proc. IEEE/CVF Conf. Comput. Vis. Pattern Recognit.*, Jun. 2018, pp. 2354–2363.

[16] H. Yao and Z. Zhang, "Research of camera calibration based on genetic algorithm BP neural network," in *Proc. IEEE Int. Conf. Inf. Autom. (ICIA)*, Aug. 2016, pp. 350–355.

[17] J.-H. Chuang, C.-H. Ho, A. Umam, H.-Y. Chen, J.-N. Hwang, and T.-A. Chen, "Geometry-based camera calibration using closed-form solution of principal line," *IEEE Trans. Image Process.*, vol. 30, pp. 2599–2610, 2021.

[18] A. E. Conrady, "Decentred lens-systems," *Monthly Notices Roy. Astronomical Soc.*, vol. 79, no. 5, pp. 384–390, Mar. 1919.

[19] T. A. Clarke and J. G. Fryer, "The development of camera calibration methods and models," *Photogramm. Rec.*, vol. 16, no. 91, pp. 51–66, Apr. 1998.

[20] F. Devernay and O. Faugeras, "Straight lines have to be straight," *Mach. Vis. Appl.*, vol. 13, no. 1, pp. 14–24, 2001.

[21] J. F. Mallon and P. Whelan, "Preciseradialun-distortion of images," in *Proc. 17th Int. Conf. Pattern Recognit. (ICPR)*, vol. 1, 2004, pp. 18–21.

[22] R. Hartley and S. B. Kang, "Parameter-free radial distortion correction with center of distortion estimation," *IEEE Trans. Pattern Anal. Mach. Intell.*, vol. 29, no. 8, pp. 1309–1321, Aug. 2007.

[23] Q. Sun, Y. Hou, and Q. Tan, "A new method of camera calibration based on the segmentation model," *Optik*, vol. 124, no. 24, pp. 6991–6995, Dec. 2013.

[24] W. Qian, J. Li, J. Zhu, W. Hao, and L. Chen, "Distortion correction of a microscopy lens system for deformation measurements based on speckle pattern and grating," *Opt. Lasers Eng.*, vol. 124, Jan. 2020, Art. no. 105804.

[25] C. Ricolfe-Viala and A.-J. Sánchez-Salmerón, "Correcting non-linear lens distortion in cameras without using a model," *Opt. Laser Technol.*, vol. 42, no. 4, pp. 628–639, Jun. 2010.

[26] C. Ricolfe-Viala and A.-J. Sánchez-Salmerón, "Using the camera pinhole model restrictions to calibrate the lens distortion model," *Opt. Laser Technol.*, vol. 43, no. 6, pp. 996–1005, Sep. 2011.

[27] G. Zhang, J. He, and X. Yang, "Calibrating camera radial distortion with cross-ratio invariability," *Opt. Laser Technol.*, vol. 35, no. 6, pp. 457–461, Sep. 2003.

[28] A. Geiger, F. Moosmann, O. Car, and B. Schuster, "Automatic camera and range sensor calibration using a single shot," in *Proc. IEEE Int. Conf. Robot. Autom.*, May 2012, pp. 3936–3943.

[29] A. J. Tabatabai and O. R. Mitchell, "Edge location to subpixel values in digital imagery," *IEEE Trans. Pattern Anal. Mach. Intell.*, vol. PAMI-6, no. 2, pp. 188–201, Mar. 1984.

[30] J. Canny, "A computational approach to edge detection," *IEEE Trans. Pattern Anal. Mach. Intell.*, vol. PAMI-8, no. 6, pp. 679–698, Nov. 1986.

CHUANG LIU received the bachelor's degree in computer science and technology from the Changchun Institute of Technology, in 2019. He is currently pursuing the master's degree in software engineering with the School of Computer Science and Technology, Changchun Normal University. His research interests include camera calibration, image processing, and 3D visual measurement.

QIUCHENG SUN received the Bachelor of Mathematics Science degree from Jilin University, in 2003, and the Ph.D. degree in mechanical engineering from the College of Mechanical Science and Engineering, Jilin University, in 2010. He is currently an Associate Professor with Changchun Normal University, China. His current research interests include camera calibration, image processing, and 3D vision measurement.

WEIYU DAI received the bachelor's degree in robotics from Beijing Union University, in 2020. He is currently pursuing the master's degree with Changchun Normal University. He is also working on the three-dimensional reconstruction of the digital gratings.

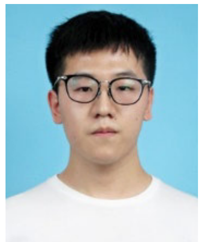

ZEMING REN is currently a Graduate Student with Changchun Normal University. His undergraduate major is in computer science and technology. His current research interests include machine vision and line structured light vision systems.

QINGLIANG LI received the Ph.D. degree from Jilin University, Changchun, China, in 2016. He is currently an Associate Professor with the College of Computer Science and Technology, Changchun Normal University. His current research interests include deep learning, image understanding, and atmospheric physics.

FANHUA YU received the B.S. degree in mathematics and applied mathematics from Changchun Normal University, Changchun, China, in 1992, and the M.S. degree in computer software and theory and the Ph.D. degree in road and railway engineering from Jilin University, Changchun, in 2004 and 2008, respectively. He is currently a Professor with the College of Computer Science and Technology, Changchun Normal University. His research interests include image processing and artificial intelligence.